Atmos. Meas. Tech. Discuss., doi:10.5194/amt-2016-14, 2016
Manuscript under review for journal Atmos. Meas. Tech.
Published: 27 January 2016

Atmospheric Measurement Techniques Discussions

Dual-polarization radar rainfall estimation in Korea according to raindrop shapes using a 2D Video Disdrometer

H. -L. Kim[1*], M.-K. Suk[1], H. -S. Park[2], G. -W. Lee[3], and J. -S. Ko[1]

[1]{Radar Analysis Division, Weather Radar Center, Korea Meteorological Administration, Seoul, South Korea}

[2]{Satellite Analysis Division, National Meteorological Satellite Center, Korea Meteorological Administration, Seoul, South Korea}

[3]{Department of Atmospheric Sciences, Kyungpook National University, Daegu, South Korea}

Correspondence to: H. -L. Kim (hlk0919@korea.kr)

Abstract

The shapes of raindrops play an important role in inducing polarimetric rainfall algorithms with differential reflectivity (Z_{DR}) and specific differential phase (K_{DP}). The shapes of raindrops have a direct impact on rainfall estimation. However, the characteristics of raindrop size distribution (DSD) are different depending on precipitation type, storm stage of development, and regional and climatological conditions. Therefore, it is necessary to provide assumptions based on raindrop shapes that reflect the rainfall characteristics of the Korean peninsula. In this study, we presented a method to find optimal polarimetric rainfall algorithms on the Korean peninsula using the 2-Dimensional Video Disdrometer (2DVD) and Bislsan S-Band dual-polarization radar. First, a new axis ratio of raindrop relations was developed for the improvement of rainfall estimation. Second, polarimetric rainfall algorithms were derived using different axis ratio relations, and estimated radar-point one-hour rain rate for the differences in polarimetric rainfall algorithms were compared with the hourly rain rate measured by gauge. In addition, radar rainfall estimation was investigated in relation to calibration bias of reflectivity and differential reflectivity. The derived raindrop axis ratio relation from the 2DVD was more oblate than existing relations in the D < 1.5 mm

Atmos. Meas. Tech. Discuss., doi:10.5194/amt-2016-14, 2016
Manuscript under review for journal Atmos. Meas. Tech.
Published: 27 January 2016

Atmospheric Measurement Techniques Discussions

and D > 5.5 mm range. The R(K_{DP}, Z_{DR}) algorithm based on a new axis ratio relation showed the best result on DSD statistics; however, the R(Z_h, Z_{DR}) algorithm showed the best performance for radar rainfall estimation, because the rainfall events used in the analysis were mainly weak precipitation and K_{DP} is noisy at lower rain rates ($\leq$ 5 mm hr^{-1}). Thus, the R(K_{DP}, Z_{DR}) algorithm is suitable for heavy rainfall and R(Z_h, Z_{DR}) algorithm is suited for light rainfall. The calibration bias of reflectivity (Z_H) and differential reflectivity (Z_{DR}) were calculated from the comparison of measured with simulated Z_H and Z_{DR} from the 2DVD. The calculated Z_H and Z_{DR} bias was used to reduce radar bias, and to produce more accurate rainfall estimation.

1 Introduction

Radar is a very useful monitoring tool for extreme weather forecasting, flood forecast and rainfall estimation because of its high spatial and temporal resolution. In particular, dual-polarization radar providing reflectivity (Z_H), differential reflectivity (Z_{DR}), differential phase (Φ_{DP}), specific differential phase (K_{DP}), and cross-correlation coefficient (ρ_{hv}) can estimate rainfall more accurately than single polarization radar. Dual-polarization radar provides characteristics of the precipitation by backscatter and differential propagation phase of hydrometeors, and therefore can obtain more information about DSD (Cifelli et al., 2011). In addition, the multi-parameters can distinguish precipitation type, and reduce the impact of DSD variability on the rainfall estimation. Therefore, rainfall estimators using a combination of Z_H, Z_{DR}, and K_{DP} are better than using reflectivity factor only (Ryzhkov et al., 2005).

Several different polarimetric rainfall algorithms have been developed assuming raindrop shapes (Sachidananda and Zrnić, 1987; Chandrasekar et al., 1990; Ryzhkov and Zrnic, 1995; Gorgucci et al., 2001). This is because the shape of raindrops is one of the most sensitive parameters for representing the DSD properties of the rain. Some researchers have attempted to produce the mean shape of raindrops. Keenan et al. (2001) derived an empirical relation from observational data, and Pruppacher and Beard (1970), Green (1975), and Beard and Chuang (1987) investigated the shape of raindrops falling under the influence of gravity. The raindrop shape is defined by the shape-size relationship of a raindrop. These raindrop axis-ratio relations play an important role in deriving polarimetric rainfall algorithms that use Z_{DR} and K_{DP} (Jameson 1983, 1985; Gorgucci et al. 2001). However, the characteristics of rain DSDs are associated with types of storms and stages of storm development as well as

Atmos. Meas. Tech. Discuss., doi:10.5194/amt-2016-14, 2016
Manuscript under review for journal Atmos. Meas. Tech.
Published: 27 January 2016

Atmospheric Measurement Techniques Discussions

climatic regimes (Bringi et al., 2003). Thus, it was necessary to determine the mean axis ratio of raindrops reflecting rainfall characteristic of the Korean peninsula, to optimize the polarimetric rainfall algorithm.

Polarization radar contains errors such as attenuation, bright band, ground clutter, and calibration bias (of Z_H and Z_{DR}). These measurement errors affect rainfall estimation. Therefore, accurate measurement and calibration of Z_H and Z_{DR} are necessary to achieve accurate radar rainfall estimation (Park and Lee, 2010). The accommodation of calibration bias of single polarimetric radar is possible by monitoring the stability of the hardware, and measured Z_H and Z_{DR} can be corrected using ground validation equipment such as a disdrometer. Joss et al. (1968) calibrated radar reflectivity using the measured Z_H from the radar profiler (at vertical incidence) and disdrometer-inferred Z_H. The radar reflectivity was calibrated by comparing reflectivity between radar and disdrometer to check the calibration of the WSR-88D (Weather Surveillance Radars—1988 Doppler) at Greer, South Carolina (Ulbrich and Lee, 1999). Goddard et al. (1982) and Goddard and Cherry (1984) compared radar with disdrometer using the axis-ratio relations of Pruppacher and Beard (1970) and Pruppacher and Pitter (1971), respectively, and found that radar measures of Z_{DR} were 0.3 dB and 0.1 dB lower than the disdrometer estimates. In addition to use of disdrometers, there are various other ways to correct biases in radar data, such as using the self-consistency constraint between Z_H and K_{DP}, vertically pointing measurements, and comparison of measured data and mean Z_H-Z_{DR} relationship (Kwon et al., 2015). Moreover, a variety of radar calibration methods were introduced in Atlas (2002).

In this study, we developed mean axis ratio relation and polarimetric rainfall algorithms using 2-Dimensional Video Disdrometer (2DVD) measurement from September 2011 to October 2012 in Daegu, Korea. The four raindrop shapes assumption [after Pruppacher and Beard (1970), Beard and Chuang (1987), and Brandes et al. (2002)] and newly derived axis-ratio relation from 2DVD data were used to derive accurate polarimetric rainfall relation for rainfall estimation. In addition, the Z_H and Z_{DR} of Bislsan dual-polarization radar were calibrated by comparing them with simulated Z_H and Z_{DR} by 2DVD. Thereafter, improvement of quantitative rainfall estimation was investigated by applying derived calibration bias. In Section 2, the data used in this study is described. The methodology for 2DVD data quality control, derived raindrop-axis ratio from 2DVD data, and simulated polarimetric parameters by the T-matrix scattering method are described in

Atmos. Meas. Tech. Discuss., doi:10.5194/amt-2016-14, 2016
Manuscript under review for journal Atmos. Meas. Tech.
Published: 27 January 2016

Atmospheric Measurement Techniques Discussions

Section 3. The results of the statistical validation of rainfall estimation are presented in Section 4. Finally, conclusions are drawn in Section 5.

2 Data and instrument

2.1 Disdrometer

The disdrometer data was used for development of mean raindrop axis ratio and polarimetric rainfall relations. The disdrometer data used in this study were measured using a 2DVD, and the data were collected from September 2011 to October 2012 in Daegu, Korea (35.9°N, 128.5°E). The 2DVD consists of two orthogonal light sheets (referred to as A and B line-scan cameras). Line-scan cameras have single-line photo detectors. The particle shadows are detected on the photo detectors and the particle images are recoded from two sides and at different heights, when particles are falling through the measurement area (10 cm × 10 cm). A more detailed description of 2DVD is given in Kruger and Krajewski (2002).

The 2DVD measures drop size, fall velocity, and the shape of individual particles. From these, one can calculate precipitation DSDs including such as the rain rate, total number concentration, and water content.

2.2 Radar

The Ministry of Land, Infrastructure, and Transport (MLIT) operates the Bislsan (BSL) dual-polarization radar in Bislsan, Korea (35.7°N, 128.5°E). The BSL S-Band radar has a narrow observation range of 150 km and frequency of 2.5 min because it is used primarily for hydrological observations and flood forecasts. The BSL S-Band radar measured polarimetric parameters such as Z_H, Z_{DR}, K_{DP} and ρ_{hv} in real time. The data obtained were from six elevation angles (from −0.5° to 1.6°), with a gate size resolution of 125 m and radar beam width of 0.95°. The specifications of the BSL radar are shown in Table 1.

The BSL S-Band dual-polarization radar is located about 22.3 km (17°) away from the 2DVD location (Fig. 1). These geographical locations were adopted to compare the two sets of observation data. We used radar data from September 2011 to October 2012. During this period, rainfall events were analyzed for products of calibration bias of Z_H and Z_{DR} and

Atmos. Meas. Tech. Discuss., doi:10.5194/amt-2016-14, 2016
Manuscript under review for journal Atmos. Meas. Tech.
Published: 27 January 2016

Atmospheric Measurement Techniques Discussions

rainfall estimation. In addition, the 0.0° plan position indicator (PPI) radar data were used to avoid effects from beam blocking and ground echoes on the measurements. The Z_H, Z_{DR}, Φ_{DP}, and ρ_{hv} radar parameters were averaged over five successive gate size resolutions and two adjacent azimuth angles, and K_{DP} was calculated from the filtered Φ_{DP} as the slope of a least squares fit.

2.3 Rain gauge

A tipping bucket rain gauge was used to validate rainfall calculated from 2DVD data. The bucket size of the rain gauge was 0.2 mm and time resolution was 0.5 s. The rain gauge was installed in the same location as the 2DVD.

3 Methodology

3.1 Quality control of 2DVD

The 2DVD observation data is useful to investigate the characteristics of rainfall. However, a number of particle outliers were measured due to wind turbulence, splashing, break up of drops, and mismatching between camera A and B (Raupach and Berne, 2015). These results lead to incorrect information about the particles. Therefore, before using the 2DVD data, a quality control process was needed.

Figures 2a and b show fall velocity and oblateness distribution according to raindrop diameter before data quality control was performed. For comparison, we plotted the axis-ratio-diameter relation of Pruppacher and Beard (1970). Some of the outliers of fall velocity and oblateness distribution were beyond the normal distribution. In particular, the outliers appeared prominently in the small raindrop ranges. To remove these outliers, velocity-based filtering was applied to the 2DVD measurement data (Thurai and Bringi, 2005).

$$|V_{measured}(D) - V_A(D)| < 0.4V_A(D)$$

$$V_A(D) = 9.65 - 10.3\exp(-0.6D) \quad (1)$$

where, D [mm] is the drop diameter, $V_{measured}$ [ms^{-1}] is the fall velocity as measured by the 2DVD, and V_A represents the Atlas velocity formula (Atlas et al. 1973). Despite the application of velocity-based filtering, significant bias still remained in the small drop size area. This was due to instrumental limitations, such as mismatch problems with the line-scan

Atmos. Meas. Tech. Discuss., doi:10.5194/amt-2016-14, 2016
Manuscript under review for journal Atmos. Meas. Tech.
Published: 27 January 2016

Atmospheric Measurement Techniques Discussions

cameras and the limited vertical resolution of the instrument. Therefore, the oblateness data corresponding to raindrop diameters smaller than 0.5 mm were removed when we calculated the new axis-ratio formula. The values outside the normal distribution (about 17%) were removed as a result of application filtering (Fig. 2c).

To analyze the reliability of the 2DVD data, we compared the rain rate calculated from the 2DVD data (Eq. 2) to collocated rain gauge measurements. The difference of accumulated rainfall represents the percent error (Eq. 3).

$$R = 6 \times 10^{-4}\pi \sum_{D_{min}}^{D_{max}} D^3 V(D) N(D) \Delta D \quad [mm\ hr^{-1}] \tag{2}$$

$$PE = \frac{|AR_{rain\ gauge} - AR_{2DVD}|}{AR_{rain\ gauge}} \times 100 \quad [\%] \tag{3}$$

here D_{max} and D_{min} are the maximum and minimum diameters of the observed drops in mm, N(D) is the drop number concentration in $mm^{-1}m^{-3}$, V(D) is the drop fall velocity in ms^{-1}, and ΔD is drop interval (ΔD = 0.2 mm). The drop fall velocity formula was derived by Brandes et al. (2002); *PE* is the percent error, and *AR* is accumulated rainfall in mm.

During the period from September 2011 to October 2012, the rainfall cases were analyzed and an example of six cases is shown in Fig. 3. The six events are (i) 0000–0900 UTC 14 October 2011, (ii) 1400–2359 UTC 2 April 2012, (iii) 0000–2359 UTC 21 April 2012, (iv) 0000–0800 UTC 25 April 2012, (v) 0000–2359 UTC 23 August 2012, and (vi) 1600–2359 UTC 27 August 2012. Figure 3a shows the accumulated rainfall computed from the 2DVD and rain gauge on 14 October 2011. The overall distribution between the 2DVD and rain gauge was good. The 2DVD recorded 13.14 mm and rain gauge recorded 13.52 mm, their difference was about 2.81%. As shown in Fig. 3b–f, percent errors from the five rainfall cases are 9.42, 0.24, 4.16, 7.88 and 8.25%, respectively. Generally, some papers show that rainfall differences between disdrometer and rain gauge were mostly from 10% to 20% (McFarquhar and List, 1993; Sheppard and Joe, 1994; Hagen and Yuter, 2003; Tokay et al., 2003). These differences might result from such issues as differences in instruments, effects from the measurement environment, and rainfall variability. Therefore, the 2DVD data within 20% percent error were used in this study.

After the quality control process, a total of 33 rainfall cases were selected for investigating the characteristics of rainfall over the Korea Peninsula. The accuracy of 33

Atmos. Meas. Tech. Discuss., doi:10.5194/amt-2016-14, 2016
Manuscript under review for journal Atmos. Meas. Tech.
Published: 27 January 2016

Atmospheric Measurement Techniques Discussions

rainfall cases was in the range of 0.24–19.32% compared to in suit rain gauges. The dataset consisted of 15 stratiform rainfall cases, 12 convective rainfall cases, and 6 mixed rainfall cases (total of 33 rainfall event) with 17,618 min DSD samples. The type of precipitation, difference rainfall, and accumulated rainfall between 2DVD and rain gauge for the 33 rainfall events are listed in Table 2. Figure 4 shows hourly and total accumulated rainfall of 2DVD and rain gauge for the 33 rainfall cases. The overall rainfall distribution between 2DVD and rain gauge were good, total accumulated rainfall by rain gauge was larger than 2DVD by about 0.81%.

3.2 Raindrop axis ratio

A very small raindrop has an approximately spherical shape that becomes oblate as its size increases. The shape of a raindrop according to drop size can be expressed as the mean axis-ratio relation; this relation is one of the most sensitive parameters for representing the rainfall properties. Hence, in order to produce rainfall estimation algorithms reflecting rainfall characteristic of the Korean peninsula, the new mean axis-ratio relation, using the 2DVD data listed in Table 2, was derived as a polynomial function. Although the measured maximum diameter from the 2DVD could reach axis-about 8.0 mm, the mean axis-ratio fitting was established to within 7 mm in order to obtain accurate information from the appropriate data. The third-order polynomial new mean axis-ratio relation (b/a) is as follows in Eq. (4), which is reasonably extended to 7 mm.

$$b/a=0.997845-0.0208475D-0.0101085D^{2}+6.4332\times10^{-4}D^{3} \quad (0.5 \le D \le 7 \text{ mm}) \quad (4)$$

where, a and b are the major axis and minor axis, respectively. D is the raindrop diameter in mm.

3.3 Disdrometer-rainfall algorithms

In order to produce the polarimetric rainfall algorithms, the theoretical polarimetric parameters (e.g., Z_H, Z_{DR}, and K_{DP}) were simulated from the 2DVD data using the T (transition) matrix method. Polarimetric parameters were simulated by making assumptions about the shape of the raindrops. First, we calculated the complex scattering amplitudes of

Atmos. Meas. Tech. Discuss., doi:10.5194/amt-2016-14, 2016
Manuscript under review for journal Atmos. Meas. Tech.
Published: 27 January 2016

Atmospheric Measurement Techniques Discussions

raindrops at the S-Band of wavelength 10.7 cm using mean axis-ratio relations. Second, calculated scattering amplitudes about the axis ratio relations were used for production of polarimetric parameters. The dual-polarimetric parameters were calculated using the following Eq. (5–7) (Jung et al., 2010).

$$Z_h = \frac{4\lambda^4}{\pi^4|K_w|^2}\int_0^{D_{max,x}} A|f_a(\pi)|^2 + B|f_b(\pi)|^2 + 2CRe[f_a(\pi)f_b^*(\pi)]N(D)dD\ [mm^6m^{-3}] \quad (5)$$

$$Z_v = \frac{4\lambda^4}{\pi^4|K_w|^2}\int_0^{D_{max,x}} B|f_a(\pi)|^2 + A|f_b(\pi)|^2 + 2CRe[f_a(\pi)f_b^*(\pi)]N(D)dD\ [mm^6m^{-3}] \quad (6)$$

Where

$$A =< cos^4\Phi >= \frac{1}{8}(3 + 4cos2\bar{\emptyset}e^{-2\sigma^2} + cos4\bar{\emptyset}e^{-8\sigma^2})$$

$$B =< sin^4\Phi >= \frac{1}{8}(3 - 4cos2\bar{\emptyset}e^{-2\sigma^2} + cos4\bar{\emptyset}e^{-8\sigma^2})$$

And

$$C =< sin^2\Phi cos^2\Phi >= \frac{1}{8}(1 - cos4\bar{\emptyset}e^{-8\sigma^2})$$

$$K_{DP} = \frac{180\lambda}{\pi}\int_0^{D_{max}} C_k Re[f_a(0) - f_b(0)]N(D)dD\ [°km^{-1}] \quad (7)$$

where $C_k =< cos2\Phi >= cos2\Phi e^{-2\sigma^2}$.

where, $f_a(0)$ and $f_b(0)$ are complex forward-scattering amplitudes, and $f_a(\pi)$ and $f_b(\pi)$ are complex backscattering amplitudes for polarization along the major and minor axes. Here, f_a^* and f_b^* are their respective conjugates, $\bar{\emptyset}$ is mean canting angle, and σ is standard deviation of the canting angle. The terms $\bar{\emptyset}$ and σ are assumed to be 7° and 0°, respectively (Huang et al., 2008). D_{max} is 7 mm, the radar wavelength is λ = 10.7 cm (S-Band), the dielectric factor for water is K_w = 0.93, and N(D) was calculated using the 2DVD measurement.

Polarimetric rainfall relations between R and dual-polarimetric parameters are derived when rain rate is greater than 0.1 mm hr^{-1}. Derived new polarimetric rainfall relations according to axis ratio relations are presented in Table3.

Atmos. Meas. Tech. Discuss., doi:10.5194/amt-2016-14, 2016
Manuscript under review for journal Atmos. Meas. Tech.
Published: 27 January 2016

Atmospheric Measurement Techniques Discussions

3.4 Calibration of radar

The polarimetric radar contains systematic bias of the radar itself. Therefore, accommodation of the calibration bias of radar is necessary to improve quantitative precipitation estimation. The calibration of the radar was done for light rainfall events, and the new axis-ratio relation (Eq. 4) was used for simulation of the theoretical Z_H and Z_{DR} parameters.

The calibration bias of Z_H and Z_{DR} were calculated from the comparison of measured Z_H and Z_{DR} with the simulated Z_H and Z_{DR} from the 2DVD measurement. To compare polarimetric radar parameters, the cross-match point must first be determined. This is, because 2DVD data are point measurements and radar data are volume measurements. The BSL S-Band radar data were averaged over five successive gates and two adjacent azimuth angles centered on the 2DVD location. The elevation angle of 0.0° PPI was used.

4 Results

4.1 Comparison of raindrop axis ratio relations

We compared the new axis-ratio experimental fit with existing mean axis-ratio relations such as those of Pruppacher and Beard (1970), Beard and Chuang (1987), and Brandes et al. (2002) in Fig. 5. These have been approximated to various polynomial formulas, as follows:

$$b/a = 1.03 - 0.062D \qquad (1 \le D \le 9 \text{ mm}) \qquad (8)$$

$$b/a = 1.0048 + 5.7\times10^{-4}D - 2.628\times10^{-2}D^2 + 3.682\times10^{-3}D^3 - 1.677\times10^{-4}D^4 \qquad (1 \le D \le 7 \text{ mm}) \qquad (9)$$

$$b/a = 0.9951 + 0.02510D - 0.03644D^2 + 5.303\times10^{-3}D^3 - 2.492\times10^{-4}D^4 \qquad (1 \le D \le 8 \text{ mm}) \qquad (10)$$

Equation 8 from Pruppacher and Beard (1970) is a linear relation from wind tunnel data, Eq. (9) is a fourth-order polynomial formula to the numerical model. Equation 10 is a polynomial empirical relation developed by Brandes et al. (2002) that was derived by combining drop shape observations. The Pruppacher and Beard (1970) linear relation (Eq. (8), green dash-dot line) falls below the new mean axis-ratio for $1 \le D < 5$ mm, and the Beard and Chuang (1987) polynomial relation (Eq. (9), black dashed line) is slightly lower than the result of the new mean axis-ratio in the range 2.5–6.5 mm. The new mean axis-ratio fit is more oblate than the

Atmos. Meas. Tech. Discuss., doi:10.5194/amt-2016-14, 2016
Manuscript under review for journal Atmos. Meas. Tech.
Published: 27 January 2016

Brandes et al. (2002) polynomial empirical relation (Eq. (10), blue dotted line) when the raindrop sizes are greater than 5.5 mm and less than 2.5 mm. To the exclusion of this part, the new axis ratio of raindrops in the range 3–5.5 mm was similar to Eq. (10).

Thus, the new mean axis ratio relation is very similar to existing axis-ratio relations except for small particles (≤ 2 mm) and large particles (≥ 5.5 mm). This means that raindrops in South Korea are more oblate than the others. Although the difference in the axis ratio seems small, its impact on the rainfall estimation cannot be neglected.

4.2 Verification of polarimetric rainfall algorithms

4.2.1 Variability of DSD in rainfall estimation

To investigate the variability of DSD in rainfall estimation from polarimetric parameters, rain rate R_e was estimated from various combinations of polarimetric variables and compared with R from Eq. (2). The mean absolute error (MAE), the root-mean-square error (RMSE), and correlation coefficient (Corr.) are defined by the following equation:

$$MAE = \frac{1}{N}\sum|R - R_e| \quad [mm\ h^{-1}] \tag{11}$$

$$RMSE = \left(\frac{1}{N}\sum(R - R_e)^2\right)^{0.5} \quad [mm\ h^{-1}] \tag{12}$$

$$\text{Corr.} = \frac{1}{N-1}\frac{\sum[(R - \bar{R})(R_e - \overline{R_e})]}{\sqrt{Var(R)Var(R_e)}} \tag{13}$$

where R is rain rate from observed 1-min DSDs and R_e is rain rate from estimated various combination of polarimetric parameters. R_e is then obtained from the same dataset. The N is the number of comparisons. Figure 6 shows the scatterplot of R and R_e for polarimetric rainfall relations based on the new axis-ratio relation and the scatter indicates the effect of DSD variability on rain estimation. The comparison between rain rates observed R and those estimated R_e shows good overall agreement. In particular, the statistic of scatter showed the best result (MAE = 0.23 mm hr^{-1}, RMSE = 0.35 mm h^{-1} and Corr = 0.10) when using the $R(K_{DP}, Z_{DR})$ based on the new axis-ratio relation. The use of the single parameter $R(Z_H)$ results in increase of the MAE = 0.96 mm hr^{-1} and RMSE = 2.40 mm hr^{-1}, and decrease of the Corr = 0.93 when compared with other polarimetric rainfall relations. Other polarimetric

Atmos. Meas. Tech. Discuss., doi:10.5194/amt-2016-14, 2016
Manuscript under review for journal Atmos. Meas. Tech.
Published: 27 January 2016

rainfall algorithms based on mean axis-ratio relations showed similar results. Thus, the polarimetric parameters with K_{DP} and Z_{DR} from dual-polarization radar reduce the DSD variability in the rainfall estimation. A summary of statistics according to polarimetric rainfall algorithms and mean axis-ratio relations are presented in Table 3.

4.2.2 Validation of rainfall estimation

In order to evaluate radar rainfall estimation according to different rainfall relations and raindrop shapes, we compared an estimated one-hour rain rate from the BSL S-Band radar to the hourly rain rate by rain gauge in Daegu, Korea. In addition, the rainfall estimate from the 2DVD was included for comparison. Statistical validation of the radar and 2DVD rainfall estimates for the different rainfall relations were performed for 18 rainfall events among the 33 rainfall cases. The mean absolute error (MAE) and the root-mean-square error (RMSE) are given by

$$MAE = \frac{1}{N}\sum |R_R - R_G| \quad [mm\ h^{-1}] \tag{12}$$

$$RMSE = \left(\frac{1}{N}\sum (R_R - R_G)^2\right)^{0.5} \quad [mm\ h^{-1}] \tag{13}$$

where, R_R is the averaged one-hour rain rate [mm h^{-1}] for the radar (or 2DVD), and R_G is the averaged one-hour rain rate [mm h^{-1}] for the rain gauge. The results are presented in Table 4.

Rainfall estimation from the 2DVD showed good results in the following order: $R(K_{DP}, Z_{DR}) > R(Z_h, Z_{DR}) > R(K_{DP}) > R(Z_h)$. According to the DSD statistics, the combined polarimetric rainfall relations using Z_{DR} and K_{DP} performed better than the single rainfall relation for estimated rainfall. As can be seen from Table 4, $R(K_{DP}, Z_{DR})$ based on the new axis-ratio relation performed better on DSD statistics, with MAE = 0.61 mm hr^{-1}, and RMSE = 0.86 mm hr^{-1}. However, the $R(K_{DP}, Z_{DR})$ algorithm showed the worst results for radar rainfall estimation, and the $R(Z_h, Z_{DR})$ algorithm showed the best performance. These results can be found in Fig. 7, which shows a scatterplot of the one-hour rain rate from the rain gauge and the radar (or 2DVD) data, using the new axis-ratio relation for 18 rainfall events. The plus represents one-hour gauge rain rate versus radar rain rate from different rainfall relations and the square indicates gauge versus 2DVD rain rate.

Atmos. Meas. Tech. Discuss., doi:10.5194/amt-2016-14, 2016
Manuscript under review for journal Atmos. Meas. Tech.
Published: 27 January 2016

Atmospheric Measurement Techniques Discussions

According to the DSD results, K_{DP} is less sensitive to DSD variation and uncertainties in raindrop shapes; however, the accuracy of the rainfall estimation declined when the K_{DP} parameter was used for radar rainfall estimation. Moreover, the radar rainfall estimations from $R(K_{DP})$ and $R(K_{DP}, Z_{DR})$ exceeded rainfall gauge measurements at lower rain rates ($\leq$ 5 mm hr^{-1}), whereas rainfall estimations from $R(Z_h, Z_{DR})$ were similar to rainfall by measured by gauges. In addition, the radar rainfall estimations from $R(K_{DP})$ and $R(K_{DP}, Z_{DR})$ perform better than those of $R(Z_h, Z_{DR})$ for rain rates exceeding 5 mm hr^{-1}. In other words, as the rain rate increased, the uncertainty of K_{DP} from the radar declined. This was because K_{DP} is noisy in light rainfall. Thus, the $R(K_{DP}, Z_{DR})$ relation is best used for heavy rainfall and $R(Z_h, Z_{DR})$ is suited for light rainfall.

In addition, the polarimetric rainfall relations based on the new axis-ratio relation also were better than the others. Although the difference in the value of the statistics seems small according to raindrop axis ratio relations, it has an effect on the accuracy of rainfall estimation. Therefore, rainfall characteristics should be reflected in polarimetric rainfall relations.

4.2.3 Correction of calibration bias

In this study, the calibration bias of Z_H and Z_{DR} was calculated for eight rainfall events, and the $R(Z_h, Z_{DR})$ algorithm based on Eq. (4) was used to estimate rainfall. Figure 8 and 9 shows comparison of the time series and scatter diagrams of Z_H and Z_{DR} for the 2DVD and BSL radar. The overall distribution of the observed Z_H corresponded well with the simulated parameter; however, the measured Z_{DR} at BSL was underestimated compared to the simulated Z_{DR} value. The mean bias (= bias) of Z_H and Z_{DR} on 14 May 2012 was about 2.17 dBZ and 0.28 dB, respectively (Fig. 8). The bias of Z_H and Z_{DR} on 23 August 2012 was 0.98 dBZ and 0.10 dB (Fig. 9).

The accuracy of the radar rainfall estimation was investigated by applying calculated Z_H and Z_{DR} bias. These results were evaluated by comparing with rain gauge measurements. Figure 10a shows the one-hour rain rate (left ordinate) and accumulated rainfall (right ordinate) estimated from the radar and rain gauge on May 14, 2012. The blue and green solid lines are estimated one-hour rainfall rates from before and after bias correction, and the bar graph is the one-hour rainfall rate measured by rain gauge. The blue and green dotted lines

Atmos. Meas. Tech. Discuss., doi:10.5194/amt-2016-14, 2016
Manuscript under review for journal Atmos. Meas. Tech.
Published: 27 January 2016

Atmospheric Measurement Techniques Discussions

are estimated accumulated rainfall from before and after bias correction, and the red dotted line is the accumulated rainfall by the rain gauge. In comparison with the rain gauge measurement, underestimated precipitation (12.67 mm) was corrected to 15.33 mm after bias correction. When the estimated rainfall was compared to the rain gauge as ground truth, rainfall estimation was improved about 13.71%. Figure 10b shows the results for the period 00:00 to 23:59 UTC on August 23, 2012. The accumulated rainfall recorded was 83.86, 71.52, and 80.12 mm for the rain gauge, before bias correction, and after bias correction. Rainfall estimation was improved about 10.25%. For eight rainfall events, the total mean bias of Z_H and Z_{DR} from the BSL radar was 1.03 dBZ and 0.22 dB, respectively. Moreover, MAE fell by 1.03 to 0.93 mm hr^{-1} and RMSE decreased by 1.41 to 1.26 mm hr^{-1}. The bias of Z_H and Z_{DR}, MAE and RMSE results for each of the eight rainfall events are presented in Table 5. As shown in Table 5, rainfall estimation tended to improve after bias correction.

5 Conclusion

The purpose of this study was to find an optimal polarimetric rainfall algorithm using 2DVD measurement in Korea, and to improve rainfall estimation by correcting Z_H and Z_{DR} calibration bias. First, we derived a new raindrop axis-ratio relation reflecting rainfall characteristics on the Korean peninsula, using data from 33 rainfall events, after checking the accuracy and quality control of the 2DVD measurements. The derived raindrop axis-ratio relation was compared with existing relations. Although the difference in relations seems small, its impact on the polarimetric rainfall algorithm cannot be neglected.

The polarimetric rainfall relations were derived based on various assumptions about the shape of raindrops, and the accuracy validation of one-hour rainfall rate for rainfall algorithms was conducted using 2DVD, BSL radar, and rain gauge. As a result, $R(K_{DP}, Z_{DR})$ based on the new axis-ratio relation was suited for rainfall estimation of the DSD statistic when compared with others. However, the K_{DP}-based algorithms had a large statistical error for radar rainfall estimation, and $R(Z_h, Z_{DR})$ based on the new axis-ratio relation showed the best performance on BSL S-Band radar rainfall estimation. This was because the measured K_{DP} parameter was weak at lower rain rates ($\leq$ 5 mm hr^{-1}). To calculate the calibration bias of radar, measured Z_H and Z_{DR} were compared with those simulated. Calculated Z_H and Z_{DR} bias was used to reduce radar bias, and to produce more accurate rainfall estimation. After bias correction, rainfall estimated from radar was close to that measured using the rain gauge.

Atmos. Meas. Tech. Discuss., doi:10.5194/amt-2016-14, 2016
Manuscript under review for journal Atmos. Meas. Tech.
Published: 27 January 2016

Atmospheric Measurement Techniques Discussions

In this paper, different axis ratios of raindrops were used to derive new polarimetric rainfall relations, and the new polarimetric rainfall algorithms were assessed for point radar rainfall estimation. The effect of areal rainfall estimation and classification of rain rate on polarimetric rainfall relations will be studied in future work.

Acknowledgements

This research was supported by the "Development and application of cross governmental dual-pol radar harmonization (WRC-2013-A-1)" project of the Weather Radar Center, Korea Meteorological Administration.

References

Atlas, D.: Radar calibration: some simple approaches, Bull. Amer. Meteor. Soc., 83, 1013-1316, 2002.

Atlas, D., Srivastava, R. C., and Sekkon, R. S.: Doppler radar characteristics of precipitation at vertical incidence, Rev. Geophys. Space Phys., 2, 1-35, 1973.

Beard, K. B., and Chuang, C.: A new model for the equilibrium shape of raindrops, J. Atmos. Sci., 44, 1509-1524, 1987.

Brandes, E. A., Zhang, G., and Vivekanandan, J.: Experiments in rainfall estimation with a polarimetric radar in a subtropical environment, J. Appl. Meteor., 41, 674-685, 2002.

Bringi, V. N., Chandrasekar, V., Zrnić, D. S., and Ulbrich, C. W.: Comments on “The need to represent raindrop size spectra as normalized gamma distributions for the interpretation of polarization radar observations, J. Appl. Meteor., 42, 1184-1189, 2003.

Chandrasekar, V., Bringi, N., Balakrishnan, and Zrnić, D. S.: Error structure of multiparameter radar and surface measurements of rainfall. Part III : Specific differential phase, J. Appl. Meteor., 32, 1288-1293, 1990.

Cifelli, R., Chandrasekar, V., Lim, S., Kennedy, P. C., Wang, Y., and Rutledge, S. A.: A New Dual-Polarization Radar Rainfall Algorithm: Application in Colorado Precipitation Events, J. Atmos. Oceanic Technol., 28, 352-364, 2011.

Goddard, J. W. F. and Cherry, S. M.: The ability of dual-polarization radar (copular linear) to predict rainfall rate and microwave attenuation, Radio Sci., 19, 201-208, 1984.

Goddard, J. W. F., Cherry, S. M, and Bringi, V. N.: Comparison of dual-polarized radar measurements of rain with ground-based disdrometer measurements, J. Appl. Meteor., 21, 252-256, 1982.

Atmos. Meas. Tech. Discuss., doi:10.5194/amt-2016-14, 2016
Manuscript under review for journal Atmos. Meas. Tech.
Published: 27 January 2016

Gorgucci, E., Scarchilli, G., Chandrasekar, V., and Bringi, V. N.: Rainfall estimation from polarimetric radar measurements: Composite algorithms immune to variability in raindrop shape-size relation, J. Atmos. Oceanic Technol., 18, 1773-1786, 2001.

Green, A. W.: An approximation for the shapes of large rain-drops, J. Appl. Meteor., 14, 1578-1583, 1975.

Hagen, M. and Yuter, S.: Relations between radar reflectivity, liquid water content, and rainfall rate during the MAPSOP, A. J. Roy. Meteor. Soc., 129, 477-493, 2003.

Huang, G. J., Bringi, V. N., and Thurai, M.: Orientation angle distributions of drops after 80m fall using a 2D video disdrometer, J. Atmos. Oceanic Technol., 25, 1717-1723, 2008.

Jameson, A. R.: Microphysical interpretation of multiparameter radar measurements in rain. Part I: Interpretation of polarization measurements and estimation of raindrop shapes, J. Atmos. Sci., 40, 1792-1802, 1983.

Jameson, A. R.: Microphysical interpretation of multiparameter radar measurements in rain. Part III: Interpretation and measurement of propagation differential phase shift between orthogonal linear polarizations, J. Atmos. Sci., 42, 607-614, 1985.

Joss, J., Thams, J. C., and Waldvogel, A.: The accuracy of daily rainfall measurements by radar, pre-prints, 13th Radar Meteorology Conf., Montreal, QC, Canada, Amer. Meteor. Soc., 448-451, 1968.

Jung. Y., Xue, M., and Zhang, G.: Simulations of polarimetric radar signatures of a supercell storm using a two-momnet bulk microphysics scheme, J. Appl. Meteor. Climatol., 49, 146-163, 2010.

Keenan, T. D., Carey, L. D., Zrnić, D. S., and May, P. T.: Sensitivity of 5-cm wavelength polarimetric radar variables to raindrop axial ratio and drop size distribution, J. Appl. Meteor., 40, 526-545, 2001.

Kruger, A., and Krajewski, W. F.:Two-dimensional video disdrometer, J. Atmos. Sci., 19, 602-617, 2002.

Kwon, S., Lee, G. W., and Kim, G.: Rainfall Estimation from an Operational S-Band Dual-Polarization Radar: Effect of Radar Calibration, J. Meteor. Soc. Japan., 93, 65-79,2015.

McFarquhar, G. M., and List, R.: The effect of curve fits for the disdrometer calibration on raindrop spectra, rainfall rate, and radar reflectivity, J. Appl. Meteor., 32, 774-782, 1993.

Park, S. –G., and Lee, G. W.: Calibration of Radar Reflectivity measurements from the KMA Operational Radar network, Asian-Pacific J. Atmos. Sci., 46, 243-259, 2010.

Pruppacher, H., and Beard, K. V.: A wind tunnel investigation of the internal circulation and shape of water drops falling at terminal velocity in air, Q. J. Roy. Meteor. Soc., 96, 247-256, 1970.

Pruppacher, H. R., and Pitter, R.: A semi-empirical determination of the shape of cloud and rain drops, J. Atmos. Sci, 28, 86-94, 1971.

Raupach, T. H., and Berne, A.: Correction of raindrop size distributions measured by parsivel disdrometers, using a two-dimensional video disdrometer as a reference, Atmos. Meas. Tech. 8, 343-365, 2015.

Ryzhkov, A. V., and Zrnić, D. S.: Comparison of dual-polarization radar estimators of rain, J. Atmos. Oceanic Technol., 12, 249-256, 1995.

Ryzhkov, A. V., Giangrande, S. E., and Schuur, T. J.: Rainfall Estimation with a Polarimetric prototype of WSR-88D, J. Appl. Meteor., 44, 502-515, 2005.

Sachidananda, M., and Zrnić, D. S.: Rain rate estimates from differential polarization measurements, J. Atmos. Oceanic Technol., 4, 588-598, 1987.

Sheppard, B. E., and Joe, P. I.: Comparison of raindrop size distribution measurements by a Joss-Waldvogel disdrometer, a PMS 2DG spectrometer, and a POSS Doppler radar, J. Atmos. Oceanic Technol., 11, 874-887, 1994.

Thurai, M. and Bringi, V. N.:Drop Axis Ratios from a 2D Video Disdrometer, J. Atmos. Oceanic Technol., 22, 966-978, 2005.

Tokay, A., Wolff, D. B., Wolff, K. R., and Bashor, P.: Rain gauge and disdrometer measurements during the keys Area Microphysics Project (KAMP), J. Atmos. Oceanic Technol., 20, 1460-1477, 2003.

Ulbrich, C. W., and Lee, L. G.: Rainfall measurement error by WSR-88D radars due to variations in Z-R law parameters and radar constant, J. Atmos. Oceanic Technol., 16, 1017-1024, 1999.

Atmos. Meas. Tech. Discuss., doi:10.5194/amt-2016-14, 2016
Manuscript under review for journal Atmos. Meas. Tech.
Published: 27 January 2016

Atmospheric Measurement Techniques Discussions

Table 1. Specification of dual-polarization radar in Bislsan.

Parameters		Characteristics
Variables		Z_H, V_r, SW, Z_{DR}, Φ_{DP}, K_{DP}, ρ_{hv}
Altitude of radar antenna		1085 m
Transmitter type		Klystron
Transmitter peak power		750 kW
Antenna diameter		8.5 m
Beam width of radar		0.95°
Observation	Frequency	2,785 MHz (S-band)
	Range	150 km
	Gate size	125 m
	Elevations	-0.5°, 0°, 0.5°, 0.8°, 1.2°, 1.6° (6 elevation)

Atmos. Meas. Tech. Discuss., doi:10.5194/amt-2016-14, 2016
Manuscript under review for journal Atmos. Meas. Tech.
Published: 27 January 2016

Atmospheric Measurement Techniques Discussions

Table 2. Summary of the date, type of precipitation, and accumulated rainfall comparison between 2DVD and rain gauge for the 33 rainfall events.

Date	Time of observation [UTC]	Type of Precipitation	Accumulated rainfall [mm]		PE [%]
			2DVD	Rain gauge	
`11.09.05	01:00-15:00	C	7.07	6.86	3.12
`11.09.09	15:20-21:20	S	4.26	4.31	1.17
`11.09.10	00:00-23:59	C	19.50	17.83	9.37
`11.09.29	00:00-17:00	S	3.81	3.72	2.38
`11.10.13	00:00-23:59	S	3.91	4.11	4.98
`11.10.14	00:00-09:00	S	13.14	13.52	2.81
`11.10.21	06:00-23:59	S	53.11	65.83	19.32
`12.04.02	14:00-23:59	M	17.79	16.26	9.42
`12.04.21	00:00-23:59	S	32.06	32.13	0.24
`12.04.25	00:00-08:00	S	18.57	17.83	4.16
`12.05.01	08:00-21:00	S	4.07	3.53	15.32
`12.05.08	07:00-11:00	C	8.98	9.60	6.50
`12.05.14	00:00-15:00	S	22.19	19.98	11.03
`12.05.28	06:00-07:00	C	15.26	14.50	5.22
`12.06.08	03:00-23:59	C	17.09	19.40	11.91
`12.06.23	00:00-08:00	C	13.48	14.50	7.05
`12.07.06	00:00-18:00	C	22.40	20.18	10.98
`12.07.12	17:00-21:00	M	7.49	7.45	0.58
`12.07.13	01:00-12:00	C	25.26	25.08	0.71
`12.07.15	00:00-12:00	C	8.22	7.64	7.55
`12.07.16	15:00-23:59	M	16.33	18.42	11.31
`12.07.21	09:00-10:30	C	5.85	5.68	2.99
`12.08.12	01:00-18:00	C	20.27	18.42	10.08
`12.08.13	00:00-15:00	C	37.19	34.09	9.10
`12.08.23	00:00-23:59	M	90.47	83.86	7.88
`12.08.24	00:00-23:59	S	7.32	7.45	1.64
`12.08.27	16:00-23:59	S	13.57	12.54	8.25
`12.08.29	19:00-23:59	S	6.23	5.29	17.72
`12.09.09	00:00-23:59	S	21.45	18.65	15.04
`12.09.16	00:00-23:59	S	82.68	69.88	18.32
`12.09.17	00:00-07:00	M	63.51	58.55	8.47
`12.10.22	06:00-11:00	M	13.60	14.92	8.81
`12.10.27	00:00-09:00	S	8.74	8.20	6.53

Atmos. Meas. Tech. Discuss., doi:10.5194/amt-2016-14, 2016
Manuscript under review for journal Atmos. Meas. Tech.
Published: 27 January 2016

Atmospheric Measurement Techniques Discussions

Table 3. List of different polarimetric rainfall relations used for rainfall estimation and MAE, RMSE and correlation coefficient for estimated rain rate vs observations.

	$R(Z_h)=\alpha\|Z_h\|^{\beta}$						
	Polarimetric rainfall relation		Scatterplot R-R_e			Assumptions
	α	β	MAE	RMSE	Corr.	
1	0.0558	0.5894	0.96	2.39	0.93	Pruppacher and Beard (1970)
2	0.0576	0.5867	0.96	2.41	0.92	Beard and Chuang (1987)
3	0.0577	0.5871	0.96	2.41	0.92	Brandes et al. (2002)
4	0.0565	0.5889	0.96	2.40	0.93	New axis ratio (Experimental fit)
	$R(K_{DP})=\alpha\|K_{DP}\|^{\beta}$					
	Polarimetric rainfall relation		Scatterplot R-R_e			Assumptions
	A	B	MAE	RMSE	Corr.	
1	38.66	0.837	0.46	1.04	0.99	Pruppacher and Beard (1970)
2	43.77	0.768	0.66	1.42	0.97	Beard and Chuang (1987)
3	46.97	0.743	0.82	1.63	0.97	Brandes et al. (2002)
4	42.28	0.833	0.45	1.14	0.98	New axis ratio (Experimental fit)
	$R(Z_h, Z_{DR})=\alpha Z_h^{\beta}10^{0.1\gamma ZDR}$					
	Polarimetric rainfall relation			Scatterplot R-R_e			Assumptions
	α	B	γ	MAE	RMSE	Corr.	
1	0.0110	0.89	-4.0808	0.45	0.77	0.99	Pruppacher and Beard (1970)
2	0.0091	0.88	-3.5197	0.46	0.83	0.99	Beard and Chuang (1987)
3	0.0088	0.88	-3.4789	0.47	0.85	0.99	Brandes et al. (2002)
4	0.0112	0.87	-3.7613	0.48	0.89	0.99	New axis ratio (Experimental fit)
	$R(K_{DP}, Z_{DR})=\alpha K_{DP}^{\beta}10^{0.1\gamma ZDR}$						
	Polarimetric rainfall relation			Scatterplot R-R_e			Assumptions
	α	β	γ	MAE	RMSE	Corr.	
1	66.23	0.96	-1.3859	0.29	0.44	0.10	Pruppacher and Beard (1970)
2	83.78	0.93	-1.6703	0.44	0.66	0.10	Beard and Chuang (1987)
3	96.37	0.92	-1.8938	0.58	0.85	0.99	Brandes et al. (2002)
4	74.54	0.97	-1.5328	0.23	0.35	0.10	New axis ratio (Experimental fit)

Atmos. Meas. Tech. Discuss., doi:10.5194/amt-2016-14, 2016
Manuscript under review for journal Atmos. Meas. Tech.
Published: 27 January 2016

Atmospheric Measurement Techniques Discussions

Table 4. Mean absolute error and root mean square error of the radar estimates of hourly rain rate for the different radar rainfall algorithms listed in Table 3.

	$R(Z_H)=\alpha\|Z_H\|^\beta$				
	MAE		RMSE		Assumptions
	RADAR	2DVD	RADAR	2DVD	
1	1.02	0.95	1.38	1.23	Pruppacher and Beard (1970)
2	1.03	0.96	1.39	1.24	Beard and Chuang (1987)
3	1.03	0.96	1.39	1.24	Brandes et al. (2002)
4	1.02	0.95	1.39	1.23	New axis ratio (Experimental fit)
	$R(K_{DP})=\alpha\|K_{DP}\|^\beta$				
	MAE		RMSE		Assumptions
	RADAR	2DVD	RADAR	2DVD	
1	6.04	0.68	6.98	0.92	Pruppacher and Beard (1970)
2	7.69	0.74	8.63	0.99	Beard and Chuang (1987)
3	8.67	0.75	9.62	1.00	Brandes et al. (2002)
4	6.80	0.70	7.79	0.92	New axis ratio (Experimental fit)
	$R(Z_H, Z_{DR})=\alpha Z_H^\beta 10^{0.1\gamma ZDR}$				
	MAE		RMSE		Assumptions
	RADAR	2DVD	RADAR	2DVD	
1	0.88	0.65	1.20	0.90	Pruppacher and Beard (1970)
2	0.86	0.67	1.19	0.93	Beard and Chuang (1987)
3	0.87	0.71	1.21	0.99	Brandes et al. (2002)
4	0.84	0.71	1.17	0.97	New axis ratio (Experimental fit)
	$R(K_{DP}, Z_{DR})=\alpha K_{DP}^\beta 10^{0.1\gamma ZDR}$				
	MAE		RMSE		Assumptions
	RADAR	2DVD	RADAR	2DVD	
1	8.56	0.62	10.03	0.88	Pruppacher and Beard (1970)
2	11.33	0.65	13.01	0.91	Beard and Chuang (1987)
3	13.16	0.68	15.01	0.94	Brandes et al. (2002)
4	9.61	0.61	11.23	0.86	New axis ratio (Experimental fit)

Atmos. Meas. Tech. Discuss., doi:10.5194/amt-2016-14, 2016
Manuscript under review for journal Atmos. Meas. Tech.
Published: 27 January 2016

Atmospheric Measurement Techniques Discussions

Table 5. Mean absolute error and root mean square error of rainfall estimates before and after applying bias correction.

	Date	Type of precipitation	Calibration Bias		MAE [mm hr^{-1}]		RMSE [mm hr^{-1}]	
			Z_h [dBZ]	Z_{DR} [dB]	Before BC	After BC	Before BC	After BC
1	`11.10.13	S	-0.01	0.10	0.48	0.38	0.59	0.47
2	10.21	S	1.16	0.28	0.75	0.74	0.98	0.97
3	`12.04.25	S	1.40	0.43	1.31	1.26	2.00	1.89
4	05.14	S	2.17	0.28	0.58	0.43	0.80	0.59
5	08.23	M	0.98	0.10	0.80	0.64	1.33	0.91
6	09.09	S	0.44	0.18	0.73	0.67	1.16	1.07
7	09.16	S	0.90	-0.13	0.77	0.71	0.95	0.92
8	10.22	M	-1.44	-0.14	2.83	2.58	3.47	3.29
Avg			1.03	0.22	1.03	0.93	1.41	1.26

* BC : Bias Correction

Atmos. Meas. Tech. Discuss., doi:10.5194/amt-2016-14, 2016
Manuscript under review for journal Atmos. Meas. Tech.
Published: 27 January 2016

Atmospheric Measurement Techniques Discussions

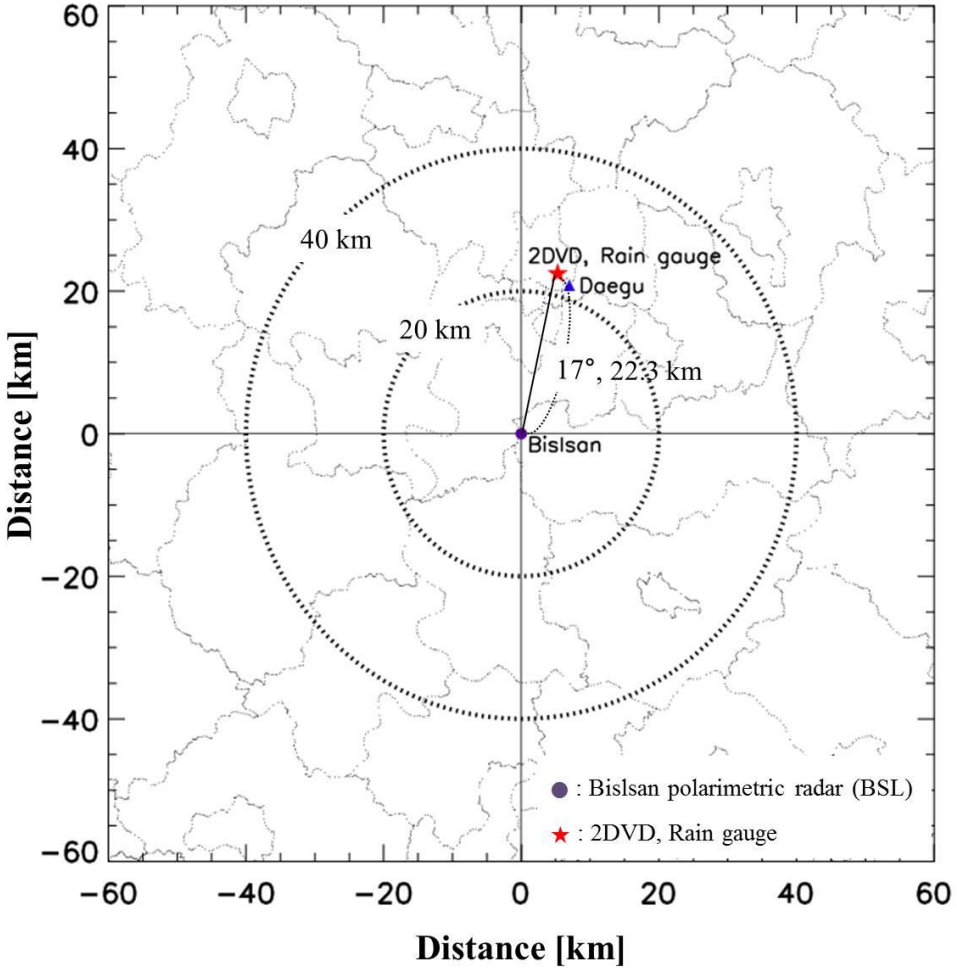

1

2 Figure 1. The location of the Bislsan polarimetric radar and the 2DVD with rain gauge site.

Atmos. Meas. Tech. Discuss., doi:10.5194/amt-2016-14, 2016
Manuscript under review for journal Atmos. Meas. Tech.
Published: 27 January 2016

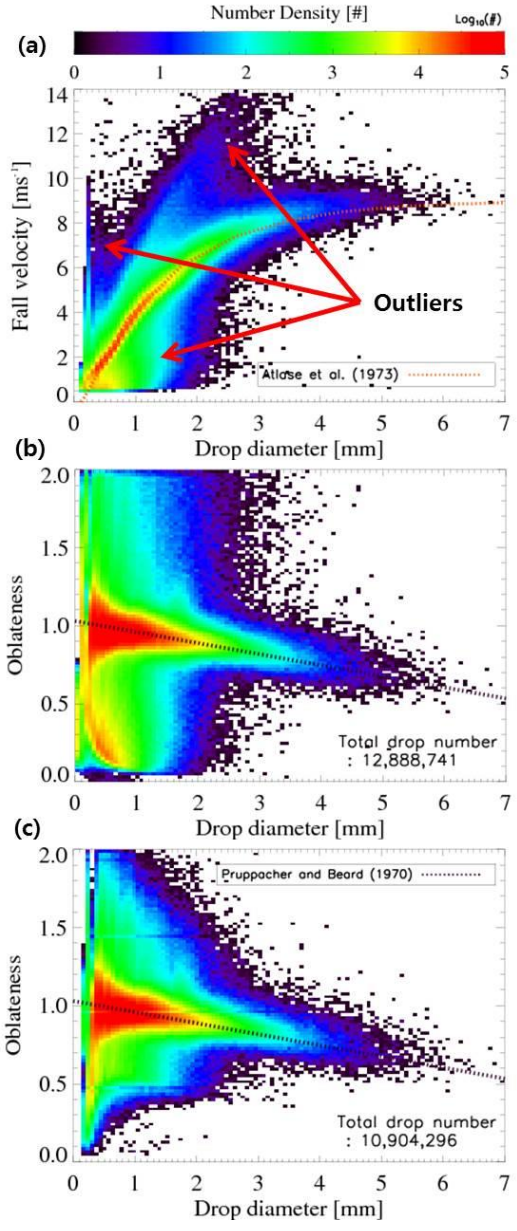

Figure 2. Distribution of fall velocity and oblateness according to drop diameter. (a) Velocity-based filter for the drop measurements. The color scale represents drop number density (log scale). (b) Drop axis ratios for all measured drops. (c) Drop axis ratios after removing mismatched drops.

Atmos. Meas. Tech. Discuss., doi:10.5194/amt-2016-14, 2016
Manuscript under review for journal Atmos. Meas. Tech.
Published: 27 January 2016

Atmospheric Measurement Techniques Discussions

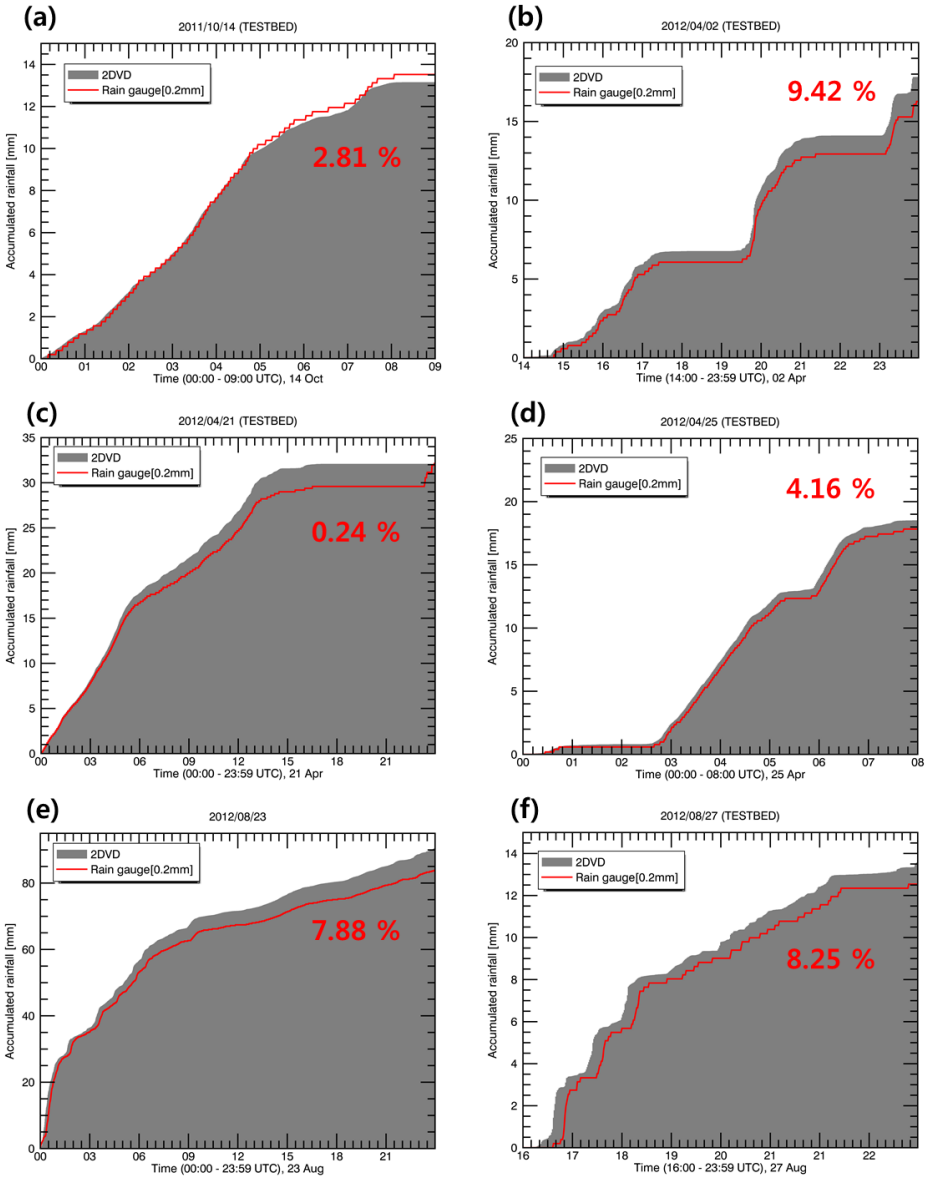

Figure 3. Time series of accumulated rainfall measured from the rain gauge and estimated from the 2DVD: (a) 14 October 2011, (b) 2 April 2012, (c) 21 April 2012, (d) 25 April 2012. (e) 23 August 2012, and (f) 27 August 2012.

Atmos. Meas. Tech. Discuss., doi:10.5194/amt-2016-14, 2016
Manuscript under review for journal Atmos. Meas. Tech.
Published: 27 January 2016

Atmospheric Measurement Techniques Discussions

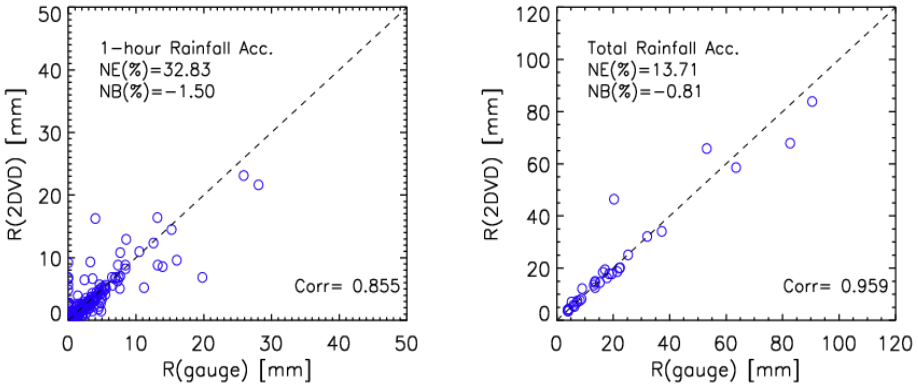

Figure 4. One-hour (left) and total accumulated rainfall (right) of 2DVD and rain gauge for the 33 rainfall cases.

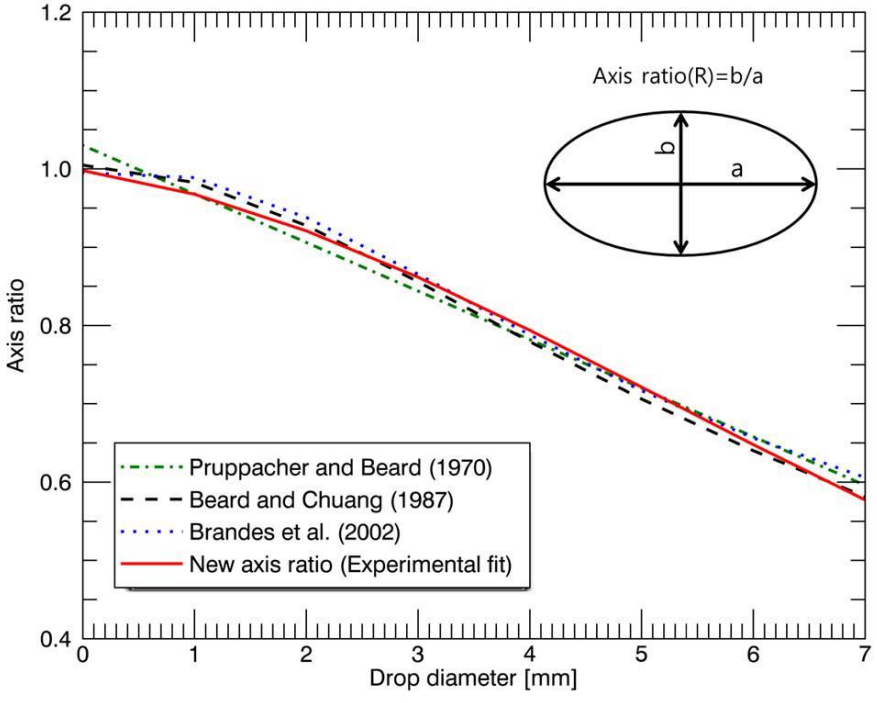

Figure 5. Different raindrop axis ratio relations for the oblate raindrop model. The upper right subfigure illustrates the axis ratio of an oblate raindrop.

Atmos. Meas. Tech. Discuss., doi:10.5194/amt-2016-14, 2016
Manuscript under review for journal Atmos. Meas. Tech.
Published: 27 January 2016

Atmospheric Measurement Techniques Discussions

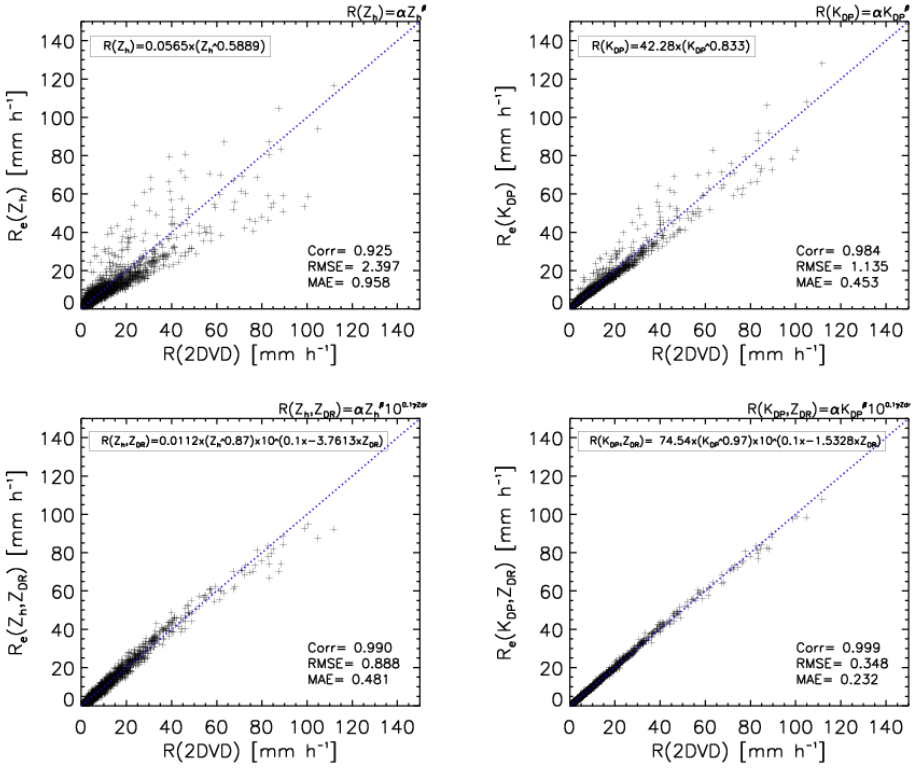

Figure 6. Scatterplot of R derived from observed DSDs of 17,618 min and R_e estimated from combinations of polarimetric parameters. R_e is then obtained from the same dataset.

Atmos. Meas. Tech. Discuss., doi:10.5194/amt-2016-14, 2016
Manuscript under review for journal Atmos. Meas. Tech.
Published: 27 January 2016

Atmospheric Measurement Techniques Discussions

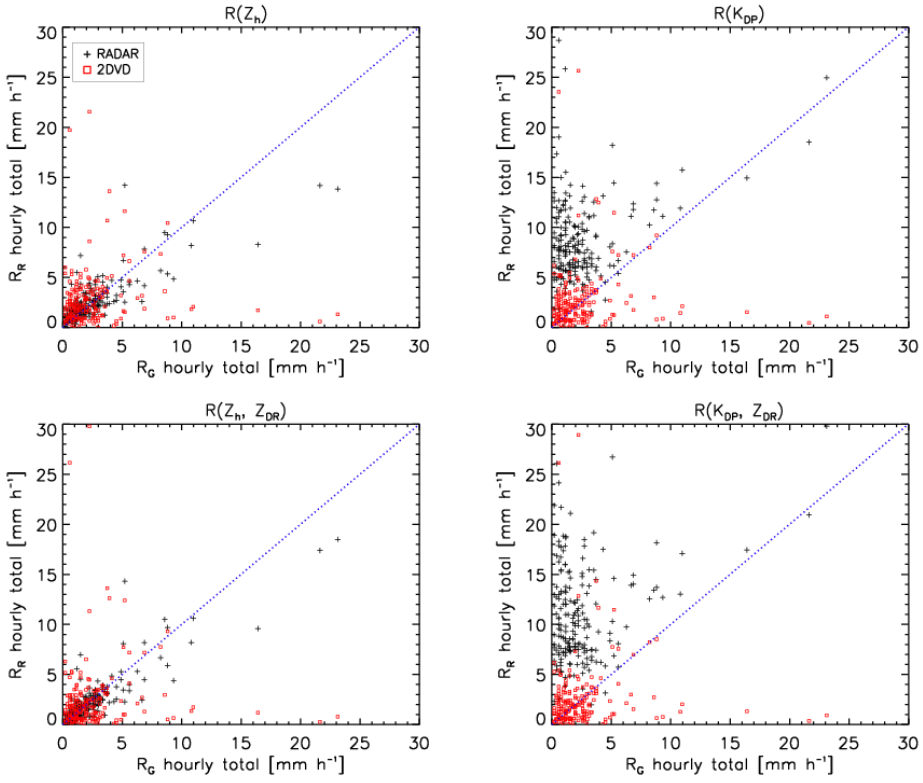

Figure 7. Scatter plot of one-hour rain rate from rain gauge (R_G) and BSL S-Band radar (or 2DVD) based on Eq. (4) for 18 rainfall cases: The pluses represents one-hour gauge rain rate versus radar hourly rain rate from polarimetric rainfall algorithms, and squares indicate gauge and 2DVD rain rate by different polarimetric rainfall algorithms.

Atmos. Meas. Tech. Discuss., doi:10.5194/amt-2016-14, 2016
Manuscript under review for journal Atmos. Meas. Tech.
Published: 27 January 2016

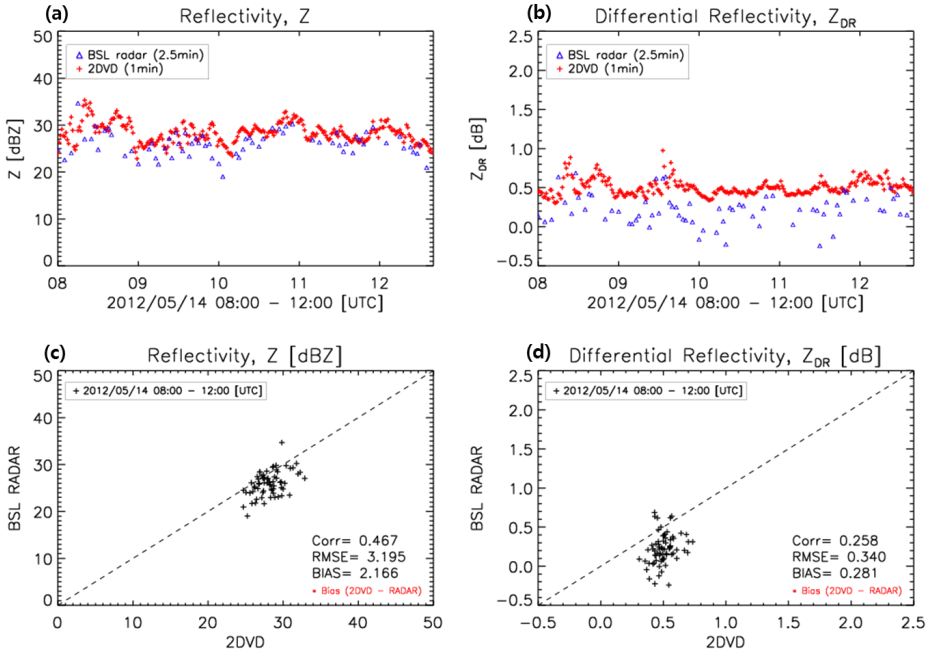

Figure 8. Time series of the (a) reflectivity, and (b) differential reflectivity by 2DVD and BSL S-Band radar: Scatter Plots of the 2DVD estimation and radar measurement for the (c) reflectivity and (d) differential reflectivity. Comparison statistics including correlation coefficient (Corr), RMSE, and bias are also presented (14 May 2012).

Atmos. Meas. Tech. Discuss., doi:10.5194/amt-2016-14, 2016
Manuscript under review for journal Atmos. Meas. Tech.
Published: 27 January 2016

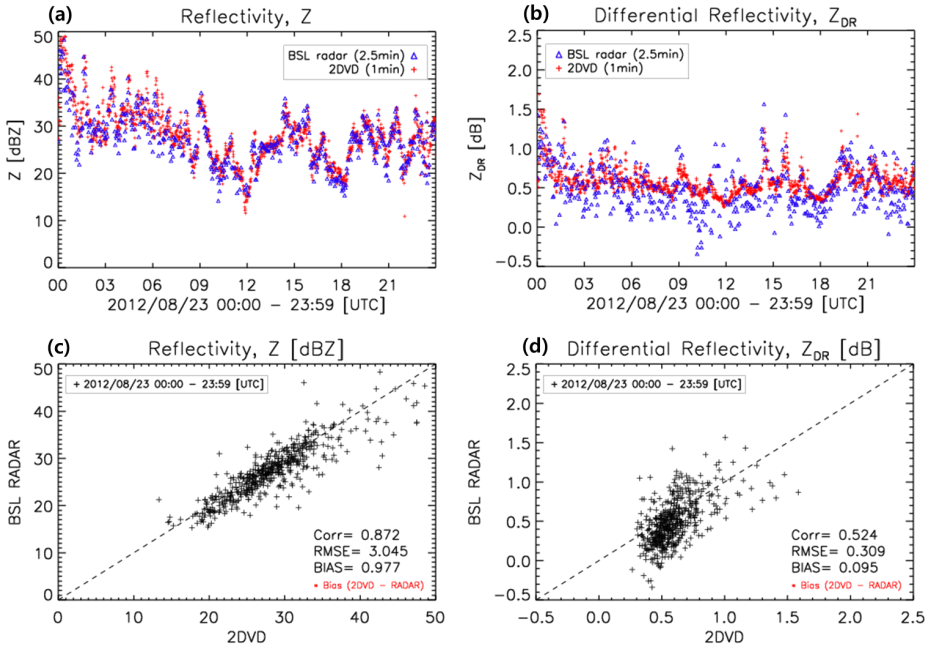

Figure 9. Same as Fig. 8, except that the data is for 23 August 2012.

Atmos. Meas. Tech. Discuss., doi:10.5194/amt-2016-14, 2016
Manuscript under review for journal Atmos. Meas. Tech.
Published: 27 January 2016

Atmospheric Measurement Techniques Discussions

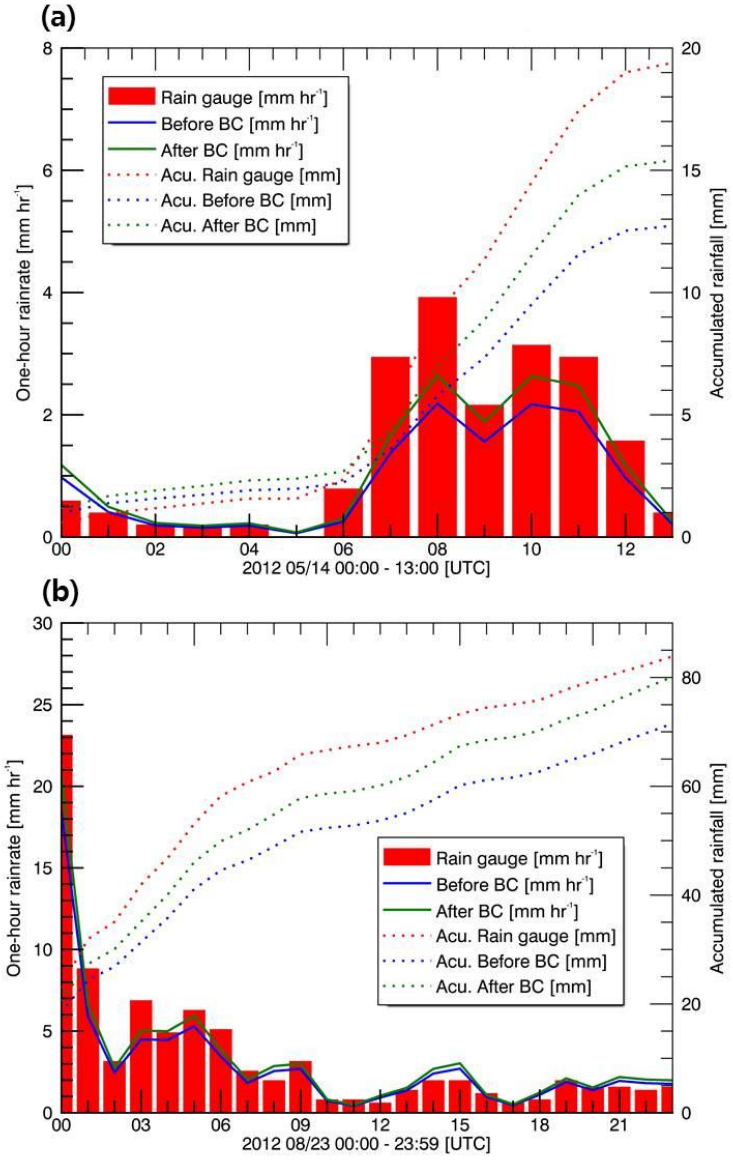

Figure 10. Comparison of the one-hour rain rate (left ordinate) and accumulated rainfall (right ordinate) obtained by BSL S-Band radar and rain gauge: The $R(Z_H, Z_{DR})$ algorithm based on Eq. (4) was used for rainfall estimation for (a) 14 May 2012 and (b) 23 August 2012. BC represents Bias Correction.